pii: sp-00728-13 http://dx.doi.org/10.5665/sleep.4246

Basal Forebrain Cholinergic Modulation of Sleep Transitions

Simal Ozen Irmak, PhD[1]; Luis de Lecea, PhD[2]

[1]Department of Biology and [2]Department of Psychiatry and Behavioral Sciences, Stanford University, Stanford, CA

Objectives: The basal forebrain cholinergic system is involved in cognitive processes that require an attentive state, an increased level of arousal, and/or cortical activation associated with low amplitude fast EEG activity. The activity of most neurons in the basal forebrain cholinergic space is tightly correlated with the cortical EEG and the activity state. While most cholinergic neurons fire maximally during waking and REM sleep, the activity of other types of basal forebrain neurons vastly differs across different arousal and sleep states. Numerous studies have suggested a role for the basal forebrain cholinergic neurons in eliciting cortical activation and arousal. However, the intricate local connectivity within the region requires the use of cell-specific manipulation methods to demonstrate such a causal relationship.

Design and Measurements: Here we have combined optogenetics with surface EEG recordings in freely moving mice in order to investigate the effects of acute cholinergic activation on the dynamics of sleep-to-wake transitions. We recorded from naturally sleeping animals and analyzed transitions from NREM sleep to REM sleep and/or wakefulness in response to photo-stimulation of cholinergic neurons in substantia innominata.

Results and Conclusions: Our results show that optogenetic activation of basal forebrain cholinergic neurons during NREM sleep is sufficient to elicit cortical activation and facilitate state transitions, particularly transitions to wakefulness and arousal, at a time scale similar to the activation induced by other subcortical systems. Our results provide in vivo cell-specific demonstration for the role of basal forebrain cholinergic system in induction of wakefulness and arousal.

Keywords: REM sleep, slow wave sleep (NREM), choline acetyltransferase (ChAT), substantia innominata (SI), nucleus basalis (NB), horizontal limb of diagonal band (HLDB), optogenetics, transgenic mice, recordings from freely moving animals, electroencephalogram (EEG)

Citation: Ozen Irmak S, de Lecea L. Basal forebrain cholinergic modulation of sleep transitions. *SLEEP* 2014;37(12):1941-1951.

INTRODUCTION

The term the basal forebrain is used to describe a number of subcortical structures rich in cholinergic neurons, including the substantia innominata, the vertical and the horizontal limbs of the diagonal band, the extended amygdala, the ventral pallidum, and the medial septum. Insults to this area, as observed in various neurodegenerative diseases such as Alzheimer disease, cause a multitude of problems in regulation of attention and arousal states, and impose devastating effects on learning and memory.[1-4] The arousal promoting effects of basal forebrain (BF) cholinergic neurons have been extensively explored in studies employing either electrical or pharmacological stimulation, or surgical or chemical ablation methods.[5-9] These studies provided strong evidence for the involvement of BF cholinergic neurons in cortical activation. However, due to the inherent limitation of the employed techniques, the lack of cell specificity of the manipulation of such a heterogeneous structure, the exact causative role of cholinergic neurons in regulation of arousal states has not yet been demonstrated.

BF cholinergic neurons are heterogeneously distributed across the medial septum, the diagonal band and the substantia innominata (SI)/nucleus basalis (NB) areas that differ in afferent and efferent connections. Cholinergic neurons constitute only a fraction[10-12] (around 5% in rats[13]) of neurons in BF, where various cell populations, including glutamatergic and different subtypes of GABAergic neurons are heterogeneously distributed across spatially distinct clusters.[14-17] Most of these neurons differ in their firing patterns and activation characteristics during sleep and/or cortical activation under anesthesia. The majority of BF cholinergic neurons increase their firing during wakefulness (and behavioral mobility) and rapid eye movement (REM) sleep,[5,18-21] as well as during spontaneous or evoked cortical activation under anesthesia.[22,23] Other neuronal cell types in BF, including GAD^+ and $ChAT^-/GAD^-$ neurons, show heterogeneous patterns of arousal state-dependent activity.[5,18-21,24] Overall, BF stimulation, likely through cholinergic activation, has been shown to modulate sensory processing[25,26] and to induce cortical activation.[27]

Given the histological and functional heterogeneity of the local circuitry, understanding the specific role of cholinergic neurons in regulation of arousal states requires the use of cell-specific manipulation methods[28-31] in naturally sleeping animals. Here we combined optogenetic manipulation and EEG recordings in freely behaving mice and explored the effects of selective activation of BF cholinergic neurons on sleep state transitions.

METHODS

All procedures followed the rules and regulations of the National Institute of Health; and were approved by the Institutional Animal Care and Use Committees at Stanford University.

Animals

Heterozygous Chat-IRES-cre mice (129S6-$Chat^{tm1(cre)Lowl}$/J, Stock number: 006410, Jackson Laboratories, Maine) backcrossed with C57BL/6J (Stock number: 000664, Jackson Laboratories, Maine) mice (20-40g, 2-5 months old male, n = 10, N3-N6 for sleep experiments and n = 2, N2 for cell-counting experiments) were used. Animals were maintained under a 12:12 light/dark cycle under constant temperature and fed ad lib.

Submitted for publication November, 2013
Submitted in final revised form May, 2014
Accepted for publication May, 2014
Address correspondence to: Luis de Lecea, 1201 Welch Road, MSLS Bld, P107, Stanford, CA 94305; Tel: (650) 736-9039; Fax: (650) 723-4655; E-mail: llecea@stanford.edu

Surgical Procedures

Animals were initially anesthetized with ketamine/xylazine (100 and 20 mg/kg, i.p., respectively) followed by hourly supplements of ketamine (100 mg/kg, i.p.). The AAV virus (0.7-0.9 μL Ef1a::DIO::eYFP or Ef1a::DIO::ChR2-eYFP, UNC Vector Core Services, NC)[32,33] was delivered either bilaterally (n = 5) or unilaterally (n = 5 for sleep recordings, n = 2 for histology) to SI (+0.02 mm AP, 1.5 mm ML and 4.5-4.7 mm DV for cell-counting, and +0.32 mm AP, 1.5 mm ML and 4.2-4.3 mm DV for behavioral experiments). A minimum of 4 weeks was allowed for viral transfection.

Histology

At the end of the experiments, animals were transcardially perfused using 4% paraformaldehyde in 0.1 M phosphate buffered saline. In order to visualize cholinergic neurons, free-floating sections were counter-stained against a cholinergic marker (1:1000, Goat Anti-ChAT Polyclonal, Millipore) and double-labeled with a fluorescent marker (1:500, Alexa Fluor 594, Donkey Anti Goat IgG, Invitrogen). Cell counting around SI/NB and horizontal limb of diagonal band (HLDB) was performed for 2 animals (16 sections with a minimum of 20 cell count per section). Viral transfection and the consistency of the cannula implantation across animals were verified in all animals by screening a minimum of 20 sections per animal. We have not observed any difference in terms of the virus expression and spread between unilateral vs. bilateral injections (n = 5 animals per group).

Stimulation

Photostimulations were performed during the light cycle (11:00-18:00 of 08:00-20:00 lights on). Either bilateral (n = 3 animals) or unilateral (n = 5 animals) 26-Gauge cannula (Plastics One, VA) and fiber system (BFL37-200, ThorLabs, NJ) was implanted in SI, such that the tip of the fiber extended to 4.7 mm from the pia mater. An additional 2 animals (one ChR2-eYFP and one eYFP) were implanted with 2-ferrule cannula system (TFC_200/260-400_5.5mm_FC_FL3, Dorics, Canada) for bilateral stimulation. Unilateral and bilateral stimulations were both statistically effective to facilitate state change ($P < 0.05$, Kolmogorov Smirnov Test), and therefore the data were pooled. Animals were 5-10 months old (with age-matched distribution across control and experimental groups) at the time of stimulation experiments. Light pulses were delivered as previously described.[31] Prior to implantation, the light output intensity at the tip of the fiber was adjusted to be 20 ± 1 mW (measurements done outside of the tissue). Different stimulation protocols of varying frequency (8-10 Hz), pulse (10-100 ms) and train duration (5-20 s) were applied across different experiments (multiple trials of the same protocol within each experiment [3-46 trials]; mostly 10-20 trials per day).

Recording

For EEG, 3 stainless steel screws were implanted above prefrontal, parietal and cerebellar cortices (for 2 animals, 4 bilateral screws over prefrontal and parietal cortices). An additional cerebellar screw was used for ground. For EMG recordings, 2 wire electrodes were bilaterally placed in the neck musculature. Differential (frontal-parietal, frontal-cerebellar and parietal-cerebellar) recordings were obtained using Grass Instruments (256 Hz sampling rate, 0.1-100 Hz band pass filtered for EEG, 0.1-3 kHz band pass filtered for EMG, Grass Technologies, RI) and Vital Recorder sleep system (Kissei Comtec America Inc., CA).

Analysis

Sleep scoring was performed using SleepSign (Kissei Comtec America Inc., CA) in 4-s windows using a combination of parameters: EEG amplitude, EMG activity, spectral power in delta, theta and alpha bands, and the continuity of the states. Episodes associated with continuous high EMG activity and/or bursts of EMG activity were considered as wakefulness. NREM states were determined by the presence of delta and/or alpha activity during highly reduced EMG activity. REM states were determined by the presence of synchronous activity at theta frequency band (4-10 Hz) coupled with flat EMG activity (muscle atonia) for a minimum of 4 s. Brief arousal states (similar to micro arousal states defined by Rolls et al.[34]) were determined by the presence of a brief period of EEG activation (0.5-2 s long, low amplitude, fast EEG), often coupled with an increased EMG activity, preceded and followed by NREM sleep.

Spectral analysis was performed on the signal derived from parietal and cerebellar electrodes; in 3 animals where such derivation was not possible, frontal-parietal derivation was used. Fast fourier transformation (FFT) was computed in 4-s windows (Hamming window, 1024 points) using built-in functions in SleepSign (Kissei Comtec America Inc., CA). After completion of sleep scoring and FFT computation, the data (sleep state, stimulation condition and spectral power of each 4-s episode) was transferred to Matlab (MatWorks, MA) computing environment. All analysis (deriving of state transition latencies and relative spectral powers, categorization of stimulations across different sleep states and durations) and figure making were performed using custom-written (to handle the pooling of data across experiments) and existing tools at Matlab environment.

To compare the impact of the ongoing sleep state on stimulation-mediated effects, stimulations applied during NREM and REM sleep were analyzed separately. NREM stimulations were further categorized into 3 groups, depending on the duration of ongoing NREM sleep prior to the stimulation onset. State transition latency was computed in terms of the number of episodes following the stimulation onset and preceding a state change.

For spectral analysis, first we computed the power (or power ratio) for each stimulation trial; then pooled the data across experiments and performed the statistics on the pooled data. (i) Mean power in each frequency bin (0.25 Hz resolution) was averaged across 5 episodes to derive 20-s preceding (PRE) and stimulation (STIM) periods. (ii) Mean power for delta (1-3.75 Hz), theta (4-9.75 Hz), alpha (10-14 Hz), gamma (20-40 Hz), slow (1-14 Hz), and wide (1-40 Hz) frequency bands were computed by first averaging the power across designated frequency bins (0.25 Hz intervals) for each episode, and then averaging the mean power across the desired time period. (iii) Relative power across PRE/STIM periods was calculated by dividing the mean power for STIM period by the mean power for PRE period. (iv) Relative power across

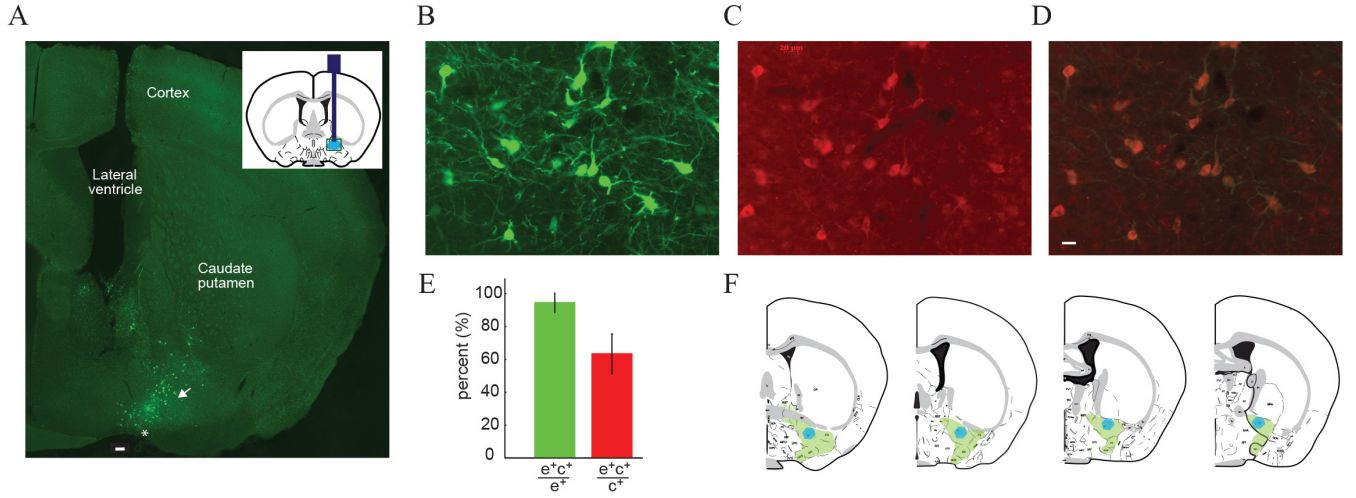

Figure 1—Cre-dependent targeting of BF cholinergic neurons. **(A)** Example of an injection and cannula implantation site in an animal injected with eYFP virus and implanted with unilateral cannula. Green, eYFP labeling. Scale is 100 micrometers. Inset, unilateral cannula placement. *Arrow head,* substantia innominata. *Asterisk,* horizontal limb of diagonal band nucleus. **(B-D)** eYFP/ChAT co-labeling around SI/NB from a coronal section around -0.08 mm AP. Scale is 20 micrometers. Zoomed in area of the green box shown in the inset in **(A)**. **(B)** eYFP labeling. **(C)** ChAT labeling. **(D)** Merged image of **(B,C)**. **(E)** Mean cell count from 2 animals (1108 cells in total). Error bars, standard deviation. Green, percent of eYFP and ChAT positive cells out of eYFP positive cells. Red, percent of eYFP and ChAT positive cells out of ChAT positive cells. **(F)** Summary schematics showing eYFP positive cells (green colored area) and fiber location (blue colored area) across animals. Images are from Allen Brain Atlas.[57] Left to right, coronal sections at +0.145 mm AP, -0.08 mm AP, -0.28 mm AP, -0.655 mm AP.

frequency bands was calculated by dividing the mean power of one band by the mean power of the other band for the given time period.

Statistics

Each stimulation trial was treated as an independent observation, and data across experiments were combined. Normality of the data was assessed and whenever the distribution deviated from normal ($P < 0.01$, Kolmogorov Smirnov test [KS test, Matlab]), nonparametric tests were utilized. Two-sample Kolmogorov Smirnov test (ktest2, Matlab) was used to compare cumulative probability distributions of transition latencies. Kruskal-Wallis test (kruskalwallis, Matlab) was used to compare the distribution of transition latencies between and within experimental conditions. Comparison of the spectral powers between experimental conditions was performed using Wilcoxon ranked sum test (ranksum, Matlab). Pairwise comparison of spectral powers across baseline and stimulation periods was performed using Wilcoxon signed rank test (signrank, Matlab). Correlation between transition latency and relative EEG power was investigated using Kendall's tau pairwise rank correlation test (corr, Matlab) and the least square line plotting tool (lsline, Matlab).

RESULTS

We injected an adeno associated virus (AAV5) encoding a floxed eYFP (DIO-YFP)[32,33] into SI/NB area of Chat-IRES-Cre animals (Figure 1A). These mice express cre recombinase under the control of the endogenous ChAT promoter.[35] Immunohistochemical analysis of SI (and bed nucleus of stria terminalis and ventral pallidum) and HLDB areas revealed that viral targeting was specific to cholinergic neurons, such that 94.5% ± 5.96% of eYFP positive neurons were also positive for cholinergic marker, ChAT; and 63.4% ± 12.02% of ChAT positive neurons were also positive for eYFP (Mean ± SD, 1108 cells from n = 2 animals; Figure 1B-1E).

A previous study by English and colleagues[36] showed that the activity of cholinergic neurons in the striatum can reliably be manipulated by a Cre-dependent viral-delivery method, similar to the conditions used here, and therefore we did not repeat in vitro recordings of photosensitive Chat cells. After verifying the specificity of the viral targeting, we injected DIO ChR2-eYFP or DIO eYFP virus into SI/NB cholinergic space (n = 5 per group) and implanted cannulas and electrodes for light delivery and for recording of EEG/EMG activity. Upon recovery, we investigated whether photostimulation of cholinergic neurons during naturally occurring sleep facilitates state transitions during the light (rest) cycle of the animals.

At the end of the experiment, animals were perfused and brains were sectioned to verify viral transfection and cannula location. Histological investigation (> 20 sections per animal) proved that cannula implantations were consistent across animals (centered around -0.28 mm posterior from Bregma and 1.5 mm from midline, with 0.2 mm variation in location; Figure 1F, Figure S1, supplemental material). eYFP Positive neurons and processes were visible in a wide range of sections from 0.94 mm anterior to 1.95 mm posterior from Bregma. eYFP Positive fibers heavily innervated amygdaloid structures (Figure S1E, supplemental material), bed nucleus of stria terminalis and neocortex. However, brain stem cholinergic areas, such as pedunculopontine and laterodorsal tegmental nucleus, lacked innervation by eYFP positive fibers (Figure S2, supplemental material).

During the light phase of a regular 12:12 light/dark schedule, animals go through multiple sleep cycles consisting of drowsiness, NREM sleep, REM sleep, and wakefulness or brief

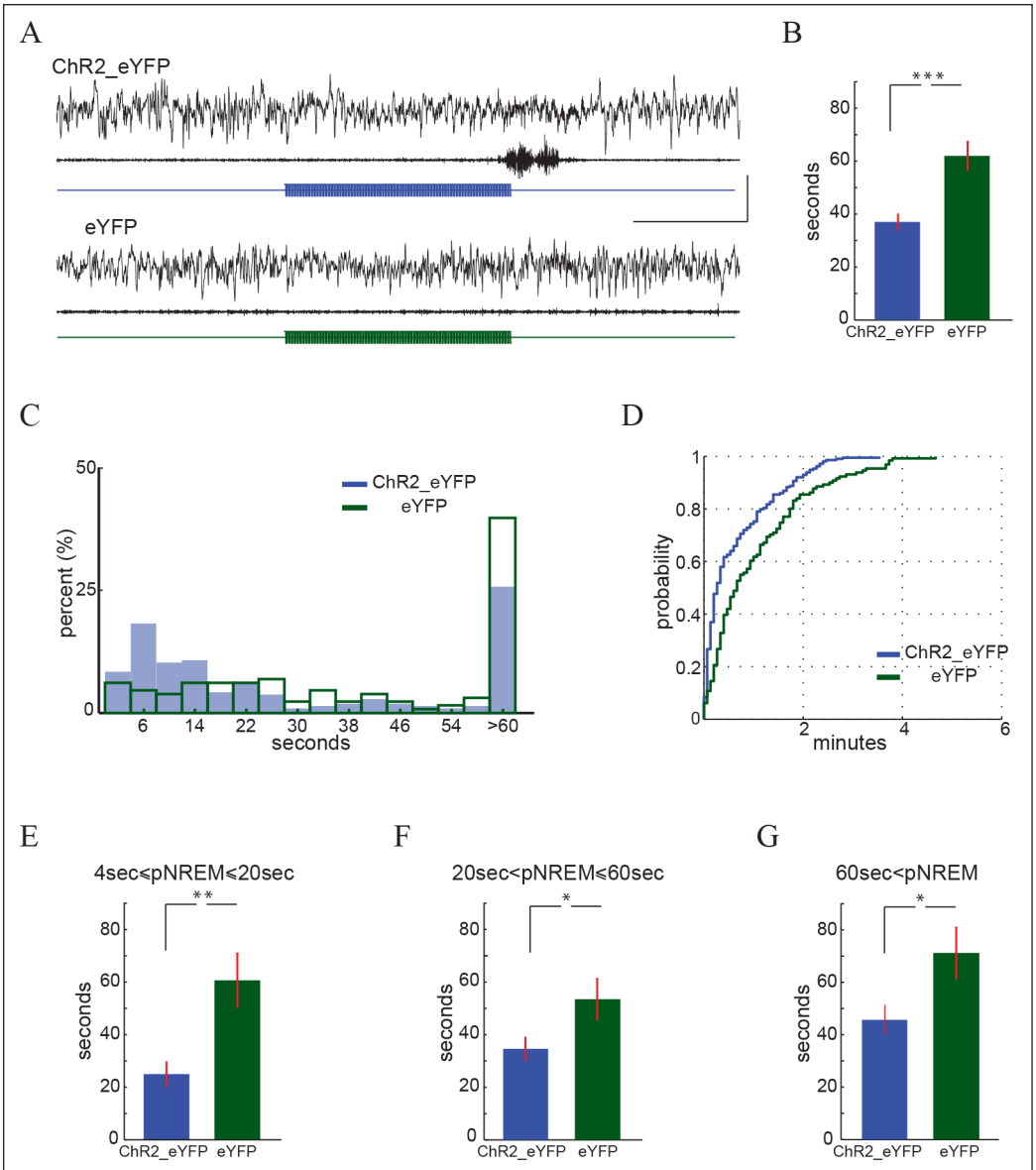

Figure 2—Effects of NREM cholinergic activation on state transitions. **(A)** Representative EEG and EMG traces preceding, during and following photo stimulation of an animal transfected with ChR2-eYFP (top 2 traces) and a control animal transfected with eYFP virus. *Scale*, 5 seconds and 0.2 mV. Stimulations were of 8 Hz frequency and applied for 10 s. **(B)** Mean (± SEM) state transition latencies. **(C)** Transition latency histogram. 4-s bins. 214 and 131 trials for ChR2-eYFP and eYFP animals, n = 5 animals per group. **(D)** Cumulative probability distribution of state transition latencies. **(E-G)** Breakdown of sessions depending on the length of preceding NREM sleep. Mean (± SEM) state transition latencies. Asterisks indicate significance according to Kruskal-Wallis test. *P < 0.05. **P < 0.001. ***P < 0.00001. Note that transition latencies are referenced to the stimulation onset. *pNREM,* prior NREM sleep episode. *ChR2_eYFP,* animals transfected with ChR2-eYFP virus. *eYFP,* animals transfected with eYFP virus.

arousal. In order to understand the effects of cholinergic activation on the naturally occurring sleep, we applied stimulations at 8-10 Hz frequency while the animal was resting in his home cage and measured the changes in sleep states, including the transition latency, the probability of a state change, the duration of transitioned states, and the changes in spectral power across delta, theta, alpha, and gamma bands. We chose stimulation rates of 8-10 Hz to mimic the average firing rates of BF cholinergic neurons (7-14 Hz during wakefulness and REM sleep;[18-20] much slower during cortical activation under anesthesia[22,23]). For technical considerations, we preferred using this mode of stimulation instead of applying phasic mode and matching > 100 Hz instantaneous firing rates.[19,20] Since cholinergic neurons decrease their activity during NREM, we particularly focused on assessing the effects of cholinergic activation during NREM sleep.

First, we checked whether stimulation affected the probability of sleep state transitions, i.e., transitions from NREM to REM sleep, to brief arousal or to wakefulness. For each stimulation trial, we calculated the transition latency, i.e., the time passed from stimulation onset to the beginning of the next sleep/arousal state. Overall, post-stimulation transitions from NREM sleep to another sleep/arousal state were much quicker for ChR2-eYFP animals than that of controls (37.0 ± 3.0 vs. 62.0 ± 5.3 s, Mean ± SEM, 214 and 131 trials for ChR2-eYFP and eYFP animals; Figure 2A-2B) and transition latencies of 2 groups were significantly different ($\chi^2(1,343) = 21.41$, P = 0.0037e-3, Kruskal-Wallis test). The probability distribution functions of both groups were also significantly different, indicating a higher probability for a state change for ChR2-eYFP animals (P = 0.0096e-3, Kolmogorov Smirnov test, 214 and 131 trials for ChR2-eYFP and eYFP groups, n = 5 animals per group; Figure 2C-2D). In a subset of experiments, stimulation was applied bilaterally (57 and 30 trials, n = 2 and n = 3 animals for ChR2-eYFP and eYFP groups). Since both unilateral and bilateral stimulations decreased the probability for state change (P < 0.05, Kolmogorov Smirnov Test), we pooled all the data for analysis. However, the majority of our results were derived from unilateral stimulations (157 and 101 trials for ChR2-eYFP and eYFP animals).

Next, we wanted to check whether, the impact of cholinergic activation depends on the timing of photostimulations with respect to the ongoing NREM episode. To address this, we applied stimulations at different time-points of NREM: (i) Within the first 20 s (early NREM stimulations), (ii) After 20 s but within the first min (mid NREM stimulations), (iii) After

60 s of NREM (late NREM stimulations). Overall, the effects on state transitions were similar across all stimulations. Regardless of the length of prior NREM sleep, cholinergic stimulation facilitated the probability of a state change (P = 0.015, P = 0.013, P = 0.02, Kolmogorov Smirnov test, 44-29, 85-51, 85-51 trials for ChR2-eYFP and eYFP groups, n = 5 animals in each group), and decreased the transition time (25.0 ± 4.6 s for early, 34.6 ± 4.4 s for mid, and 45.6 ± 5.4 s for late NREM stimulations, Mean ± SEM, P = 0.00076, P = 0.011, and P = 0.014, for early, mid, and late NREM stimulations, Kruskal-Wallis test; Figure 2E-2G). Although, early NREM stimulations seemed to have the most robust effect (P < 0.001 vs. P < 0.05), transition latencies across 3 stimulation groups were not significantly different ($\chi^2(2,211) = 5.59$, P = 0.051 for ChR2-eYFP and $\chi^2(2,128) = 1.67$, P = 0.434 for eYFP animals within group comparisons, Kruskal-Wallis test).

Following NREM stimulations, ChR2-eYFP animals transitioned into wakefulness (including brief arousal and quiet wakefulness states) at a slightly higher, but not significantly different rate (76.5% ± 3.9% vs. 68.8% ± 6.9%, Mean ± SEM percentages from 18 and 14 experiments for ChR2-eYFP and eYFP groups, n = 5 animals per group, P > 0.05, Kruskal-Wallis Test; Figure 3A). Segmenting trials according to preceding NREM length revealed a similar trend (Figure 3B). The duration of wakefulness state, directly transitioned from NREM sleep, was significantly longer for ChR2-eYFP animals compared to eYFP animals (21.4 ± 6.8 vs. 7.0 ± 0.9 seconds, Mean ± SEM, P = 0.0004, Kruskal-Wallis test, 167 and 90 trials for ChR2-eYFP and eYFP animals, n = 5 animals per group; Figure 3C).

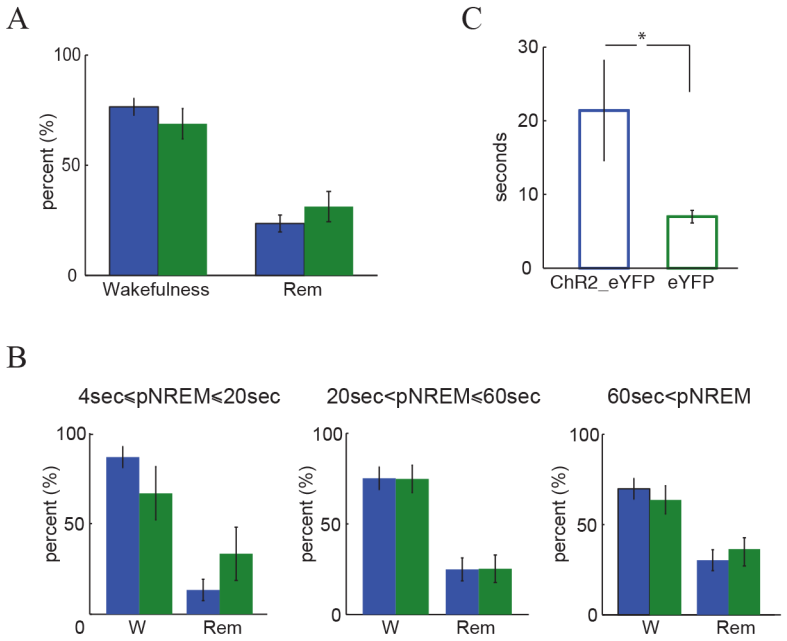

Figure 3—Post-stimulation transitioned states. **(A)** Percent of transitions to wakefulness, including brief arousal states, and REM sleep. Mean (± SEM) frequency of transitions to wakefulness was 76.5% ± 3.9% for ChR2-eYFP animals and 68.8% ± 6.9% for eYFP animals. **(B)** Same as in **(A)** but categorized according to prior NREM length. Rates of transitions to wakefulness (Mean ± SEM) were the following: 86.7% ± 5.9% for ChR2-eYFP and 66.7% ± 14.7% for eYFP animals for early NREM trials; 75.2% ± 6.4% for ChR2-eYFP and 74.7% ± 7.6% for eYFP animals for mid NREM trials; 69.8% ± 5.8% for ChR2-eYFP and 63.6% ± 7.8% for eYFP animals for late NREM trials. Blue, ChR2-eYFP animals. Green, eYFP animals. *W*, wakefulness including brief arousal states. **(C)** Duration of wakefulness, transitioned after optogenetic stimulation. Mean (± SEM) seconds. *ChR2_eYFP*, animals transfected with ChR2-eYFP virus. *eYFP*, animals transfected with eYFP virus.

In order to assess whether cholinergic activation facilitated transitions-to-wakefulness, we focused on trials where the animals directly transitioned from NREM sleep to wakefulness (including brief arousal states). In line with our previous results, we found that the probability of state transitions from NREM to wakefulness was significantly different between ChR2-eYFP and eYFP groups (P < 0.0001, Kolmogorov Smirnov test, for 167 and 90 trials, n = 5 animals per group; Figure S3A, supplemental material) with shorter transition latencies for ChR2-eYFP animals (31.5 ± 3.2 vs. 52.8 ± 6.2 s, Mean ± SEM, for ChR2-eYFP and eYFP groups, P < 0.0001, Kruskal-Wallis test; Figure S3B, supplemental material). However, parsing trials into early, mid, and late NREM stimulations revealed that the probability of NREM-to-wakefulness transitions was only affected by mid and, to a lesser significance degree, early NREM stimulations (P = 0.0284, P = 0.0034, and P = 0.089, Kolmogorov Smirnov test for 38-23, 66-37, and 63-30 trials, n = 5-4, n = 5-5, n = 5-5 animals, ChR2-eYFP and eYFP groups for early, mid, and late NREM stimulations). Likewise, transition latencies of ChR2-eYFP and eYFP animals were significantly different only for early NREM stimulations (17.9 ± 3.3 vs. 49.6 ± 11.1 s, Mean ± SEM, for ChR2-eYFP and eYFP groups, P = 0.0026 for early; 29.4 ± 4.7 vs. 46.3 ± 9.3 s, Mean ± SEM, for ChR2-eYFP and eYFP groups, P > 0.01 for mid; and 42.0 ± 6.5 vs. 63.2 ± 11.9 s, Mean ± SEM, for ChR2-eYFP and eYFP groups, P > 0.05 for late NREM stimulations, Kruskal-Wallis test; Figure S3C-S3E, supplemental material). Comparison of transition latencies across early, mid, and late NREM stimulations confirmed, albeit weakly, the difference within stimulation groups ($\chi^2(2,164) = 1.06$, P = 0.049 and $\chi^2(2,40) = 1.41$, P = 0.493 for within ChR2-eYFP and within eYFP group comparisons, Kruskal-Wallis test). These results suggested the importance of the length of ongoing NREM sleep in shaping the wakefulness inducing effects of cholinergic stimulation.

To have a better understanding of the arousing effects of cholinergic stimulation, we performed spectral analysis of EEG. In order to work on comparable time frames across trials, we focused our analysis on 20 s of periods before and after the stimulation onset (PRE, 20 s of the baseline period preceding the stimulation onset, and STIM, 20 s of the period starting with the stimulation onset). In order to ensure ChR2-eYFP and eYFP groups had a similar baseline, we compared PRE period mean power in delta, theta, and alpha bands (normalized by the mean power across 1-14 Hz) between experimental groups. The lack of significant difference (P = 0.62, P = 0.09, P = 0.06, for delta, theta, and alpha bands, 214 and 131 trials for ChR2-eYFP and eYFP groups, n = 5 animals per group, Wilcoxon ranked sum test) ensured that stimulation induced effects were not due to

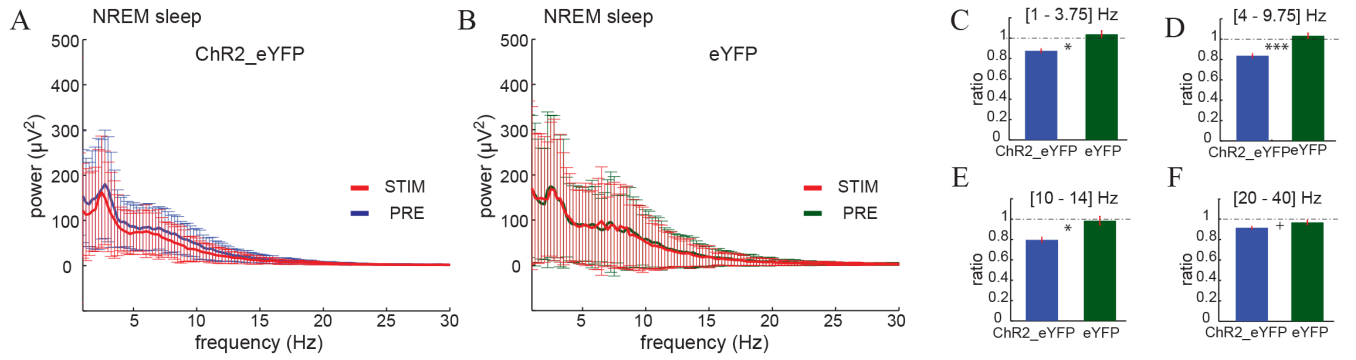

Figure 4—Effects of NREM cholinergic activation on spectral power. **(A,B)** Spectral power across baseline (PRE) and stimulation (STIM) periods for ChR2-eYFP and eYFP animals. Error bars, standard deviation. **(C-F)** STIM/PRE mean power ratios across frequency bands. Error bars, standard error of the mean. Asterisks indicate significance according to paired Wilcoxon signed rank test. $^{+}P < 0.05$. $^{*}P < 0.001$. $^{***}P < 0.00000001$. *PRE*, 20-s preceding the stimulation onset. *STIM*, 20-s after the stimulation onset.

Table 1—Correlation between state transition latency and power in delta and theta bands.

	ChR2-eYFP	eYFP
All trials and transitions with a significant (P < 0.05) correlation		
Delta	–	r = +0.131, P = 0.03470
Theta	–	r = −0.162, P = 0.00903
Delta/Theta	–	r = +0.143, P = 0.02071
All mid-NREM trials		
Delta	–	r = +0.244, P = 0.01768
Theta	–	r = −0.252, P = 0.01445
Delta/Theta	–	r = +0.237, P = 0.02152
All NREM-to-REM transitions		
Delta	–	r = +0.392, P = 0.00043
Theta	–	r = −0.374, P = 0.00078
Delta/Theta	–	r = +0.389, P = 0.00047
All mid-NREM trials of NREM-to-REM transitions		
Delta	–	r = +0.5, P = 0.01569
Theta	–	–
Delta/Theta	–	r = +0.456, P = 0.02806
All late-NREM trials of NREM-to-REM transitions		
Delta	r = +0.445, P = 0.00465	r = +0.419, P = 0.01126
Theta	r = −0.357, P = 0.02356	r = −0.366, P = 0.02713
Delta/Theta	r = +0.436, P = 0.00554	r = +0.377, P = 0.02292

Only correlations with significant relationship (P < 0.05, Kendall's tau pairwise rank correlation) are shown. Delta and theta powers are normalized by the mean power in the slow band (1-14 Hz).

any prior difference among NREM sleep states of ChR2-eYFP and eYFP animals.

Next, we compared the mean power in each frequency bin (1-40 Hz wide band signal parsed in 0.25 Hz intervals) across PRE and STIM periods. For ChR2-eYFP group, this paired analysis revealed multiple frequency bins where STIM mean power differed from that of PRE period (56 bins with P < 0.0001, 15 additional bins with P < 0.001, 21 additional bins with P < 0.01, Wilcoxon signed rank test, 214 trials, n = 5 animals). In contrast, for eYFP group, only 9 bins were significantly different across PRE and STIM periods (1 bin with P < 0.001 level, 8 additional bins with P < 0.01 level, 131 trials, n = 5 animals; Figure 4A-4B). Band-wise analysis confirmed the robust difference between STIM and PRE periods, where STIM period mean power in delta, theta, alpha, and gamma bands were lower than that of PRE period. This effect was only present for ChR2-eYFP group but not for eYFP animals (P < 0.0001e-5 for all bands for pairwise comparisons within ChR2-eYFP group vs. P > 0.01 for all within group comparisons in eYFP animals, Wilcoxon signed rank test). These effects were also visible at the combined 1-40 Hz wide band signal (P = 0.0047e-15 vs. P = 0.374 for ChR2-eYFP and eYFP groups, Wilcoxon signed rank test). Band-wise comparison of STIM period mean power normalized by PRE period mean power (STIM/PRE ratio) between ChR2-eYFP and eYFP groups confirmed the stimulation mediated decrease in delta, theta and alpha powers in ChR2-eYFP animals (P = 0.0003, P = 0.00192e-6, P = 0.00012, and P = 0.00349e-6 for delta, theta, alpha, and wide-band comparisons, P > 0.01 for gamma band, Wilcoxon ranked sum test; Figure 4C-4F).

In the next set of analyses; we focused on identifying the effects of stimulation on the EEG activity preceding a state transition. We explored pre-REM[37] and pre-wake correlates of EEG activity and evaluated whether and how cholinergic activation affected those indicators. For each stimulation trial, we defined a pre-transition period, starting with the stimulation onset and ending with the start of the next sleep/arousal state, which was determined by the initial sleep scoring. Then, we checked the correlations between pre-transition period mean powers across delta and theta bands with state transition latencies. Observations from eYFP control animals provided the benchmarked comparison for the physiological condition. Overall, all correlations were very weak (the strongest correlation being r = −0.252, 131 trials, n = 5 animals for eYFP animals; Table 1). Cholinergic stimulation further abolished these weak relationships (214 trials, n = 5 animals). We then divided trials into 2 categories based on the transitioned state, REM vs. wakefulness (including brief arousal states). In control animals, we found relatively stronger correlations between transition latency to REM and normalized delta, theta, and delta/theta ratio (r = 0.39, r = −0.37, and r = 0.39, P < 0.001, 40

trials from n = 4 eYFP animals). These correlations were more robust for longer NREM bouts (for mid and late-NREM trials where prior NREM is > 20 s), where delta and theta powers, as well as delta/theta ratio were all correlated with REM sleep transition latency (|r| > 0.36 for late-NREM trials, 21 trials, n = 4 eYFP animals, P < 0.05, Kendall tau pairwise rank-correlation test; Table 1, Figure 5). At first glance, such a correlation was absent for ChR2-eYFP group (P > 0.05, 45 trials, n = 5 ChR2-eYFP animals). However, when trials were parsed according to prior NREM length, we discovered relatively stronger correlations for ChR2-eYFP animals (|r| > 0.35, P < 0.05, 22 trials, n = 5 animals) for late NREM trials. These findings provide further support to the sleep-state dependent effects of cholinergic activation. Early and mid NREM stimulations, which induced wakefulness, disrupted the correlation while late NREM stimulations did not disrupt the correlation, nor induced wakefulness, instead they might have facilitated the imminent transitions to REM sleep. Overall, we could not find any robust EEG correlate of preceding wakefulness, neither in eYFP nor in ChR2-eYFP animals (83 trials and 151 trials, n = 5 animals per group, for eYFP and ChR2-eYFP animals, P > 0.05, Kendall tau pairwise rank-correlation test).

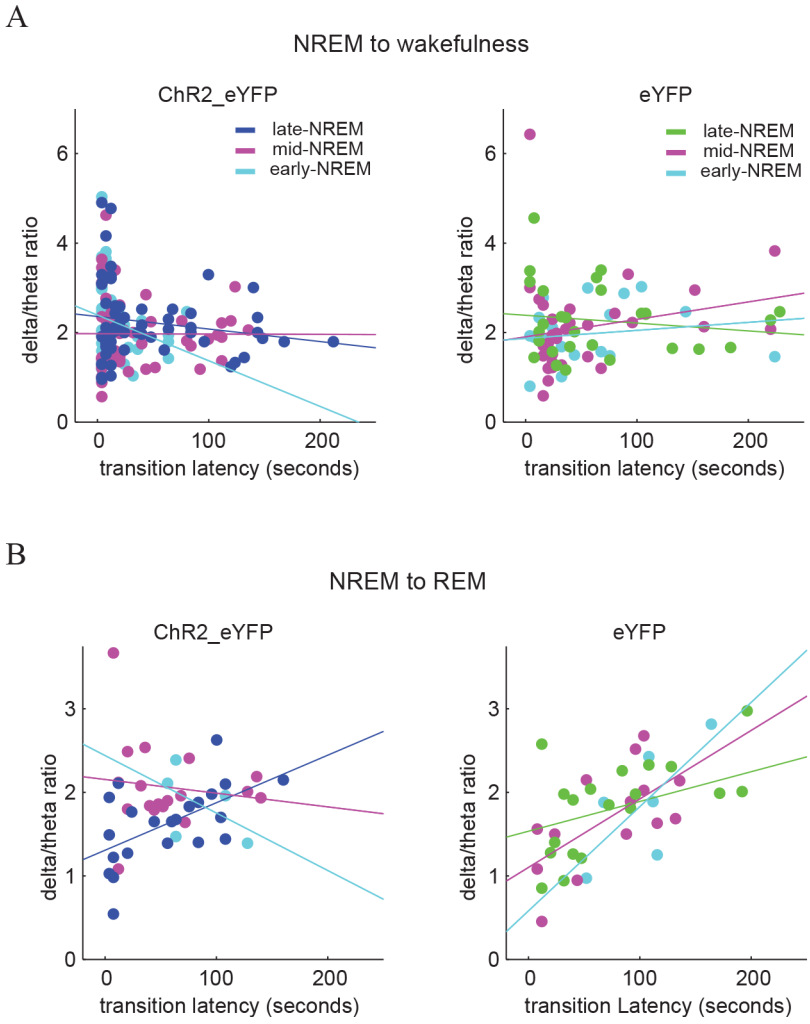

Figure 5—EEG correlates of state transitions. **(A,B)** Correlation between pre-transition period delta/theta power and the transition latency to wakefulness **(A)** and to REM sleep **(B)** separately shown for ChR2-eYFP (left column) and eYFP (right column) groups. Color of the markers indicates the length of prior-NREM sleep (i.e., early, mid, late NREM trials). Blue/green, prior NREM was > 60 s. Magenta, prior NREM was > 20 s and < 60 s. Cyan, prior NREM was < 20 s. Legend applies to all subplots.

Neocortical, hippocampal, and subcortical neuronal activities (including basal forebrain cholinergic neurons) vastly differ across NREM and REM sleep states. In order to test the effects of sleep states on stimulation-mediated arousal, in a subset of experiments, we applied stimulations during REM sleep. Photostimulation of cholinergic neurons during REM did not affect the probability of state transitions (P > 0.05, Kolmogorov Smirnov test, 45 and 18 trials, n = 4 and n = 3 animals, for ChR2-eYFP and eYFP groups; Figure 6A). State transition latencies, were also not different between the 2 groups (47.20 ± 6.83 vs. 39.78 ± 10.40 s, Mean ± SEM, for ChR2-eYFP and eYFP animals, P > 0.05, Kruskal-Wallis test). It should be noted that relatively short nature of the REM sleep makes it hard to delineate finer scale effects of stimulation from the naturally occurring differences in neural activity across REM cycle. Regardless, the comparison of STIM/PRE mean power ratios between ChR2-eYFP and eYFP animals did not reveal any difference across any of the frequency bands (P > 0.05 for delta, theta, alpha, gamma, and wide-band comparisons, Wilcoxon ranked sum test; Figure 6B-6C).

When the stimulations were applied during active wakefulness (Figure S4, supplemental material), we did not observe any disruption to the behavior of the animal or any pathological activity across the EEG. Pairwise comparisons of spectral activity in trials presented no significant difference among pre-stimulation and pre-transition (stimulation) periods for either of the experimental groups (P > 0.01 for all band-wise comparisons, i.e., delta, theta, alpha, gamma, wide band comparisons, Wilcoxon signed rank test, 14 and 10 trials for ChR2-eYFP and eYFP groups, n = 3 animals per group). However, we would like to emphasize the limitation of our analysis due to the limited scope of our study, not including satisfactory number of trials for wake behaving assessments.

DISCUSSION

We showed that optogenetic activation of BF cholinergic neurons during NREM sleep is sufficient to facilitate transitions to wakefulness and arousal. Several authors have previously shown that optogenetic targeting of cholinergic system is a reliable manipulation method to induce behavioral and electrophysiological effects.[36,38,39] We also have shown that natural sleep of animals can be manipulated to induce wakefulness and/or to fragment sleep by the use of optogenetic tools.[31,33,34,40] A study by Han and colleagues[41] was published during the revision of this report,

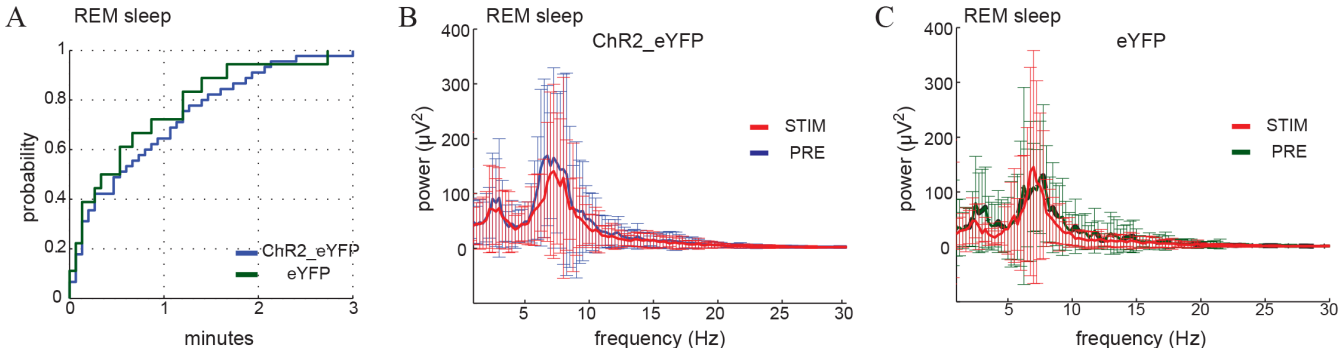

Figure 6—Optogenetic stimulation during REM sleep. **(A)** Cumulative probability distribution of state transition latencies. **(B,C)** Spectral power across baseline (PRE) and stimulation (STIM) periods for ChR2-eYFP and eYFP animals. Error bars, standard deviation. *PRE*, 20-s preceding the stimulation onset. *STIM*, 20-s after the stimulation onset.

demonstrating the arousal inducing effects of optogenetic activation of cholinergic neurons and fibers within BF.

Several studies suggest the existence of different populations of BF cholinergic neurons that might differ in terms of firing properties and anatomical projections.[14,39] This diversity may also exist in the membrane molecules involved in viral delivery and might explain the rather incomplete targeting, approximately 60%, of cholinergic neurons using AAV based Cre approach as applied here. However, the observed innervations of both neocortex and amygdaloid structures by eYFP-positive neurons suggest that we could reliably recruit cholinergic neurons that vary in their projection profiles.

Optogenetic activation of cholinergic neurons during NREM sleep, disrupted the ongoing sleep state, facilitated state transitions, particularly transitions to wakefulness, and prolonged the duration of post-stimulation arousal. These effects were manifested as an overall decrease in the power across 1-14 Hz frequency band. These changes in the neocortical EEG within 20 seconds of the stimulation onset are reflective of the disruption of NREM associated neural synchrony. Moreover, cholinergic activation mediated state transitions were relatively slow to develop (~30 seconds on average) and the transitioned wakefulness states lasted longer, suggesting the recruitment of postsynaptic targets of BF cholinergic system and an overall facilitation of arousal. The absence of any observable electrophysiological abnormalities or behavioral distress supports the relevance of our findings to the physiological effects exerted by BF cholinergic neurons during natural arousal and sleep states.

In our study, optogenetic stimulations did not elicit an immediate alertness and the induced effects were not specific to the activity in theta-band. However, most of our current understanding on the subcortical arousal system is coming from the studies that used manipulation techniques with different timescales and/or selectivity characteristics (e.g., pharmacological or surgical ablation methods, electrical or pharmacological stimulations, agonist/antagonist applications to cortical targets). Our stimulations were predominantly unilateral; bilateral stimulations could have elicited more robust effects with shorter transition latencies and smaller variability across trials. In addition, not all BF cholinergic neurons were targeted; engaging a limited fraction of cholinergic neurons might have played a role, as well. Some of the differences in expected vs. observed impact might also be attributed to the stimulation differentially recruiting tonic vs. burst firing modes of cholinergic neurons.[18-20,22,42] Although, 10 Hz stimulation was shown to elicit burst firing in BF cholinergic neurons in vitro,[41] our 8-10 Hz stimulation might not have elicited burst firing, which can reach more than 100 Hz frequencies within bursts.[18-20] Our stimulation might have also elicited a "wake-like" cholinergic tone since cholinergic neurons fire, on average, 7 Hz during active wake and 14 Hz during REM sleep (rates are slower for cortical activation elicited in anesthetized preparations).[18-20,22,23] It is also possible that 10 Hz stimulation was limited in its effectiveness in inducing arousal.[41] Future studies that would combine optogenetics with in vivo intracortical recordings from BF cholinergic neurons would help to clarify the underlying physiology of the induced effects.

Our findings and the recently published findings by Han and colleagues[41] are similar regarding the following aspects: (1) Han et al. reported a "frequently observed immediate" state transition that occurred within 15 seconds from the onset of the stimulation, which was applied 12 seconds after NREM onset. This effect is similar to our early NREM trials, where the stimulation induced wakefulness with a mean latency of 18 seconds. (2) Both studies showed that stimulations applied during REM sleep did not induce arousal or wakefulness. (3) The breakdowns of transitioned wakefulness and REM states are also similar (80% to 20% ratio vs. 76.5% to 23.5% ratio). (4) In terms of the spectral analysis, peak frequencies were not shifted by the stimulation. The overall effect (decrease in power) on slow frequencies reported in our study is similar to the reported decrease in power of 7-10 Hz range by Han et al. The difference in timeframes of EEG analysis conducted in both studies disables a more detailed one-to-one comparison.

Despite the similarities, our findings diverge from the recent report in two main areas: (1) The shorter duration of induced wakefulness reported by Han and colleagues[41] contrasts with our observations. (2) The increased probability of the continuation (and the duration) of REM sleep reported by Han et al. is different than our report of the lack of change on the transition probability and the mean state transition latency (i.e., the duration of sustained REM sleep). Stimulation and analysis related differences could be one potential explanation of these differences. Han and colleagues' stimulations were applied after 12

seconds of state onset; this is similar to our early NREM trials but constitutes a different condition than that of our remaining NREM trials, where we sampled the effects of stimulation applied at longer lengths of the ongoing sleep state. Moreover, some of their quantification was based on the trials that "induced a state transition within 15 seconds" and some of their comparisons were based on the previous day's sleep. We employed a different approach where we included all trials, regardless of the presumed effectiveness of a given stimulation trial; and our comparison was based on what was observed in strain-matched control animals. Another possibility to explain the differences might be the use of different frequency stimulations. Despite both frequency stimulations elicit similar burst firing in vitro,[41] 8-10 Hz frequency applied in our study might have recruited neurons/fibers in a way different than that of 20 Hz frequency did. Nevertheless, the main methodical difference between our study and Han et al. is the use of transgenic animals and the method of viral delivery. Considering BF cholinergic neurons are not the only source of cholinergic input to BF, it is critical to ensure that other cholinergic neurons, particularly the projection fibers of brain stem cholinergic nuclei[43-47] are not activated. In our case, viral expression was limited to the injection site, SI/NB and HLDB area, ensuring that the stimulation activated only the cell body and fibers of these neurons. Moreover, in our study, only a subpopulation (60%) of the targeted neurons expressed ChR2. In other words, our targeting was specific but limited to a subpopulation of cholinergic neurons within BF region. On the other hand, Han and colleagues[41] used ChAT-ChR2-EYFP mice (ChAT mice) and had an almost complete (95%) targeting of BF cholinergic neurons. However, ChAT mice were reported to express ChR2 in cholinergic neurons of other regions, as well.[48-50] Despite the use of offspring of animals without apparent expression in LDT/PPT, cholinergic fibers bypassing and/or projecting to the area that was in the range of the stimulation could have been activated.[41] Moreover, cholinergic neurotransmission is enhanced in ChAT-mice due to the overexpression of the functional vesicular acetylcholine transporter gene.[51] The enhanced cholinergic tone was suggested to cause disruptions in learning and attention processing, enhanced motor behavior and dark cycle drinking and feeding activities observed in these mice.[51] In short, the cholinergic tone recruited by the two studies was different. The combined results might be reflecting a spectrum of effects that vary depending on the pool of the recruited cholinergic tone within BF, ranging from the activation of a sub-population of BF cholinergic neurons to the activation of all cholinergic neurons and fibers within BF.

Comparison of the arousal inducing effects of BF cholinergic activation with other neuromodulatory systems studied in our laboratory[31,33,34,40] shows similarities across hypocretinergic and BF cholinergic activation. Optogenetic modulation of hypocretinergic neurons were shown to facilitate transitions to wakefulness within 35-45 seconds from the stimulation onset,[31,40] a latency similar to that observed following optogenetic stimulation of cholinergic neurons (29-38 seconds). On the other hand, activation of noradrenergic neurons in locus coeruleus mediated an almost instantaneous transition to wakefulness.[33] These differences support the notion that individual arousal promoting circuits are activated by different modulatory signals and have different contributions to the dynamics of sleep and wakefulness.[52,53]

In contrast to the hypocretin-induced awakenings,[31] the arousal promoting effects of cholinergic modulation were dependent on the ongoing sleep states, as photostimulation of cholinergic neurons during REM sleep did not increase wakefulness. Our findings also suggest that the timing of the stimulation, relative to the length of preceding NREM episode, affected the probability of state transitions (particularly the transitions to wakefulness) where wake-promoting effects of cholinergic activation were not significant for stimulations preceded by long periods of NREM. Furthermore, stimulations applied during early and mid NREM disrupted the relationship between delta/theta powers and the transition latency, particularly for NREM to REM transitions, as observed in control animals. On the other hand, for late NREM stimulations the correlation between delta/theta powers and the transitions to REM sleep was similar (with a slight increase) to that of control animals, suggesting the absence of a stimulation-induced disruption of delta/theta power and transition latency relationship. Benington and colleagues[37] have shown that the changes in delta and theta powers reliably predict the sleep state transitions; where a decrease in delta/theta ratio precedes the REM onset, while high delta/theta ratio predicts the prolonged NREM state. This relationship was disrupted for early and mid NREM trials; but not for late NREM trials. One plausible interpretation is that early and mid NREM stimulations induced transitions to wakefulness whereas late NREM stimulations played a facilitatory role for the imminent transitions to REM sleep. These effects might be a result of state-dependent cholinergic sensitivity of arousal systems. During early NREM sleep (such as after 20 s of NREM), the activity of cholinergic neurons is likely to be minimal;[18-20] this would ensure the maximum level of impact exerted by external activation of cholinergic neurons (as also shown by Han et al.[41]). On the other hand, as NREM develops and the sleep cycle comes closer to a transition period, cholinergic neurons start to join the active pool of neurons and increase their firing.[18-20] Thus, optogenetic stimulations applied at this late NREM period may not be able to produce a differential signal, enough to induce wakefulness; instead it may facilitate transitions to REM sleep, which occur more frequently after long NREM bouts.[37] Such state-dependent effects of cholinergic activation might have substantial use for therapeutic or experimental purposes, where induction of either REM sleep or wakefulness is specifically desired.

In a recent study, Yang and colleagues[50] demonstrated an additional role for BF cholinergic system to modulate cortical activation and arousal. Cholinergic inputs, originating from collaterals of neighboring BF cholinergic neurons[54,55] and/or projections from brain stem cholinergic neurons,[43-47] excited cortically projecting basal forebrain GABAergic neurons.[20,23] Disinhibition of neocortex through the activation of long-range inhibitory neurons[6,23,56] is a likely contributor to the arousal inducing effects of BF cholinergic activation observed in our study.

In our study, we focused on understanding the effects of activation of cholinergic neurons in SI/NB and HLDB areas on state transitions in naturally sleeping animals. Further studies are needed to reveal the impact of cholinergic activation in relation to sleep pressure and the homeostatic regulation, as well

as the effects of cholinergic drive on more attentive arousal states (such as encoding of sensory information during an object recognition task) and cognitive load (such as memory consolidation and/or memory retrieval). Furthermore, it would be important to extend this research to investigate the arousal promoting roles of other BF cholinergic neurons, neurons in the medial septum and/or the vertical limb of the diagonal band areas, as well as brain stem cholinergic neurons.

ACKNOWLEDGMENTS

The authors thank Dr. Juan Mena-Segovia for his feedback on the manuscript. We also thank the anonymous expert Reviewers of *SLEEP* for their diligent input and constructive comments.

DISCLOSURE STATEMENT

This was not an industry supported study. This work was supported by NIHMH. Dr. Ozen Irmak was supported by the Hilda and Preston Davis Foundation. The authors have indicated no financial conflicts of interest. The work was performed at the Department of Psychiatry and Behavioral Sciences, Stanford University, Stanford, CA.

REFERENCES

1. Whitehouse PJ, Price DL, Clark AW, Coyle JT, DeLong MR. Alzheimer disease: evidence for selective loss of cholinergic neurons in the nucleus basalis. Ann Neurol 1981;10:122-6.
2. Whitehouse PJ, Price DL, Struble RG, Clark AW, Coyle JT, Delon MR. Alzheimer's disease and senile dementia: loss of neurons in the basal forebrain. Science 1982;215:1237-9.
3. Damasio AR, Graff-Radford NR, Eslinger PJ, Damasio H, Kassell N. Amnesia following basal forebrain lesions. Arch Neurol 1985;42:263-71.
4. Zaborszky L, van del Pol A, Gyengesi E. The basal forebrain cholinergic system in mice. In: Watson C, Paxinos G, Puelle L, eds. The Mouse Nervous System. Elsevier, 2011:680-92.
5. Buzsaki G, Bickford RG, Ponomareff G, Thal LJ, Mandel R, Gage FH. Nucleus basalis and thalamic control of neocortical activity in the freely moving rat. J Neurosci 1988;8:4007-26.
6. Jimenez-Capdeville ME, Dykes RW, Myasnikov AA. Differential control of cortical activity by the basal forebrain in rats: a role for both cholinergic and inhibitory influences. J Comp Neurol 1997;381:53-67.
7. Cape EG, Jones BE. Effects of glutamate agonist versus procaine microinjections into the basal forebrain cholinergic cell area upon gamma and theta EEG activity and sleep-wake state. Eur J Neurosci 2000;12:2166-84.
8. Cape EG, Manns ID, Alonso A, Beaudet A, Jones BE. Neurotensin-induced bursting of cholinergic basal forebrain neurons promotes gamma and theta cortical activity together with waking and paradoxical sleep. J Neurosci 2000;20:8452-61.
9. Detari L. Tonic and phasic influence of basal forebrain unit activity on the cortical EEG. Behav Brain Res 2000;115:159-70.
10. Albanese A, Gozzo S, Iacopino C, Altavista MC. Strain-dependent variations in the number of forebrain cholinergic neurons. Brain Res 1985;334:380-4.
11. Kalesnykas G, Puolivali J, Sirvio J, Miettinen R. Cholinergic neurons in the basal forebrain of aged female mice. Brain Res 2004;1022:148-56.
12. Perez SE, Dar S, Ikonomovic MD, DeKosky ST, Mufson EJ. Cholinergic forebrain degeneration in the APPswe/PS1DeltaE9 transgenic mouse. Neurobiol Dis 2007;28:3-15.
13. Gritti I, Henny P, Galloni F, Mainville L, Mariotti M, Jones BE. Stereological estimates of the basal forebrain cell population in the rat, including neurons containing choline acetyltransferase, glutamic acid decarboxylase or phosphate-activated glutaminase and colocalizing vesicular glutamate transporters. Neuroscience 2006;143:1051-64.
14. Zaborszky L, Pang K, Somogyi J, Nadasdy Z, Kallo I. The basal forebrain corticopetal system revisited. Ann N Y Acad Sci 1999;877:339-67.
15. Zaborszky L, Buhl DL, Pobalashingham S, Bjaalie JG, Nadasdy Z. Three-dimensional chemoarchitecture of the basal forebrain: spatially specific association of cholinergic and calcium binding protein-containing neurons. Neuroscience 2005;136:697-713.
16. Castaneda MT, Sanabria ER, Hernandez S, et al. Glutamic acid decarboxylase isoforms are differentially distributed in the septal region of the rat. Neurosci Res 2005;52:107-19.
17. Nadasdy Z, Varsanyi P, Zaborszky L. Clustering of large cell populations: method and application to the basal forebrain cholinergic system. J Neurosci Methods 2010;194:46-55.
18. Lee MG, Manns ID, Alonso A, Jones BE. Sleep-wake related discharge properties of basal forebrain neurons recorded with micropipettes in head-fixed rats. J Neurophysiol 2004;92:1182-98.
19. Lee MG, Hassani OK, Alonso A, Jones BE. Cholinergic basal forebrain neurons burst with theta during waking and paradoxical sleep. J Neurosci 2005;25:4365-9.
20. Hassani OK, Lee MG, Henny P, Jones BE. Discharge profiles of identified GABAergic in comparison to cholinergic and putative glutamatergic basal forebrain neurons across the sleep-wake cycle. J Neurosci 2009;29:11828-40.
21. Takahashi K, Lin JS, Sakai K. Characterization and mapping of sleep-waking specific neurons in the basal forebrain and preoptic hypothalamus in mice. Neuroscience 2009;161:269-92.
22. Manns ID, Alonso A, Jones BE. Discharge properties of juxtacellularly labeled and immunohistochemically identified cholinergic basal forebrain neurons recorded in association with the electroencephalogram in anesthetized rats. J Neurosci 2000;20:1505-18.
23. Duque A, Balatoni B, Detari L, Zaborszky L. EEG correlation of the discharge properties of identified neurons in the basal forebrain. J Neurophysiol 2000;84:1627-35.
24. Manns ID, Alonso A, Jones BE. Discharge profiles of juxtacellularly labeled and immunohistochemically identified GABAergic basal forebrain neurons recorded in association with the electroencephalogram in anesthetized rats. J Neurosci 2000;20:9252-63.
25. Metherate R, Ashe JH. Basal forebrain stimulation modifies auditory cortex responsiveness by an action at muscarinic receptors. Brain Res 1991;559:163-7.
26. Metherate R, Ashe JH. Nucleus basalis stimulation facilitates thalamocortical synaptic transmission in the rat auditory cortex. Synapse 1993;14:132-43.
27. Metherate R, Cox CL, Ashe JH. Cellular bases of neocortical activation: modulation of neural oscillations by the nucleus basalis and endogenous acetylcholine. J Neurosci 1992;12:4701-11.
28. Nagel G, Szellas T, Huhn W, et al. Channelrhodopsin-2, a directly light-gated cation-selective membrane channel. Proc Natl Acad Sci U S A 2003;100:13940-5.
29. Boyden ES, Zhang F, Bamberg E, Nagel G, Deisseroth K. Millisecond-timescale, genetically targeted optical control of neural activity. Nat Neurosci 2005;8:1263-8.
30. Zhang F, Wang LP, Boyden ES, Deisseroth K. Channelrhodopsin-2 and optical control of excitable cells. Nat Methods 2006;3:785-92.
31. Adamantidis AR, Zhang F, Aravanis AM, Deisseroth K, de Lecea L. Neural substrates of awakening probed with optogenetic control of hypocretin neurons. Nature 2007;450:420-4.
32. Sohal VS, Zhang F, Yizhar O, Deisseroth K. Parvalbumin neurons and gamma rhythms enhance cortical circuit performance. Nature 2009;459:698-702.
33. Carter ME, Yizhar O, Chikahisa S, et al. Tuning arousal with optogenetic modulation of locus coeruleus neurons. Nat Neurosci 2010;13:1526-33.
34. Rolls A, Colas D, Adamantidis A, et al. Optogenetic disruption of sleep continuity impairs memory consolidation. Proc Natl Acad Sci U S A 2011;108:13305-10.
35. Lowell BB, Olson D, Yu J. Development and phenotype of ChAT-IRES-Cre mice. MGI Direct Data Submission, 2006.
36. English DF, Ibanez-Sandoval O, Stark E, et al. GABAergic circuits mediate the reinforcement-related signals of striatal cholinergic interneurons. Nat Neurosci 2011;15:123-30.
37. Benington JH, Kodali SK, Heller HC. Scoring transitions to REM sleep in rats based on the EEG phenomena of pre-REM sleep: an improved analysis of sleep structure. Sleep 1994;17:28-36.
38. Witten IB, Lin SC, Brodsky M, et al. Cholinergic interneurons control local circuit activity and cocaine conditioning. Science 2010;330:1677-81.

39. Unal CT, Golowasch JP, Zaborszky L. Adult mouse basal forebrain harbors two distinct cholinergic populations defined by their electrophysiology. Front Behav Neurosci 2012;6:21.
40. Carter ME, Adamantidis A, Ohtsu H, Deisseroth K, de Lecea L. Sleep homeostasis modulates hypocretin-mediated sleep-to-wake transitions. J Neurosci 2009;29:10939-49.
41. Han Y, Shi YF, Xi W, et al. Selective activation of cholinergic basal forebrain neurons induces immediate sleep-wake transitions. Curr Biol 2014;24:693-8.
42. Khateb A, Muhlethaler M, Alonso A, Serafin M, Mainville L, Jones BE. Cholinergic nucleus basalis neurons display the capacity for rhythmic bursting activity mediated by low-threshold calcium spikes. Neuroscience 1992;51:489-94.
43. Woolf NJ, Butcher LL. Cholinergic systems in the rat brain: III. Projections from the pontomesencephalic tegmentum to the thalamus, tectum, basal ganglia, and basal forebrain. Brain Res Bull 1986;16:603-37.
44. Hallanger AE, Wainer BH. Ascending projections from the pedunculopontine tegmental nucleus and the adjacent mesopontine tegmentum in the rat. J Comp Neurol 1988;274:483-515.
45. Semba K, Reiner PB, McGeer EG, Fibiger HC. Brainstem afferents to the magnocellular basal forebrain studied by axonal transport, immunohistochemistry, and electrophysiology in the rat. J Comp Neurol 1988;267:433-53.
46. Jones BE, Cuello AC. Afferents to the basal forebrain cholinergic cell area from pontomesencephalic--catecholamine, serotonin, and acetylcholine--neurons. Neuroscience 1989;31:37-61.
47. Losier BJ, Semba K. Dual projections of single cholinergic and aminergic brainstem neurons to the thalamus and basal forebrain in the rat. Brain Res 1993;604:41-52.
48. Ren J, Qin C, Hu F, et al. Habenula "cholinergic" neurons co-release glutamate and acetylcholine and activate postsynaptic neurons via distinct transmission modes. Neuron 2011;69:445-52.
49. Zhao S, Ting JT, Atallah HE, et al. Cell type-specific channelrhodopsin-2 transgenic mice for optogenetic dissection of neural circuitry function. Nat Methods 2011;8:745-52.
50. Yang C, McKenna JT, Zant JC, Winston S, Basheer R, Brown RE. Cholinergic neurons excite cortically projecting basal forebrain GABAergic neurons. J Neurosci 2014;34:2832-44.
51. Kolisnyk B, Guzman MS, Raulic S, et al. ChAT-ChR2-EYFP mice have enhanced motor endurance but show deficits in attention and several additional cognitive domains. J Neurosci 2013;33:10427-38.
52. Carter ME, Brill J, Bonnavion P, Huguenard JR, Huerta R, de Lecea L. Mechanism for hypocretin-mediated sleep-to-wake transitions. Proc Natl Acad Sci U S A 2012;109:E2635-44.
53. de Lecea L, Carter ME, Adamantidis A. Shining light on wakefulness and arousal. Biol Psychiatry 2012;71:1046-52.
54. Zaborszky L, Heimer L, Eckenstein F, Leranth C. GABAergic input to cholinergic forebrain neurons: an ultrastructural study using retrograde tracing of HRP and double immunolabeling. J Comp Neurol 1986;250:282-95.
55. Zaborszky L, Duque A. Local synaptic connections of basal forebrain neurons. Behav Brain Res 2000;115:143-58.
56. Freund TF, Meskenaite V. γ-Aminobutyric acid-containing basal forebrain neurons innervate inhibitory interneurons in the neocortex. Proc Natl Acad Sci U S A 1992;89:738-42.
57. Lein ES, Hawrylycz MJ, Ao N, et al. Genome-wide atlas of gene expression in the adult mouse brain. Nature 2007;445:168-76.

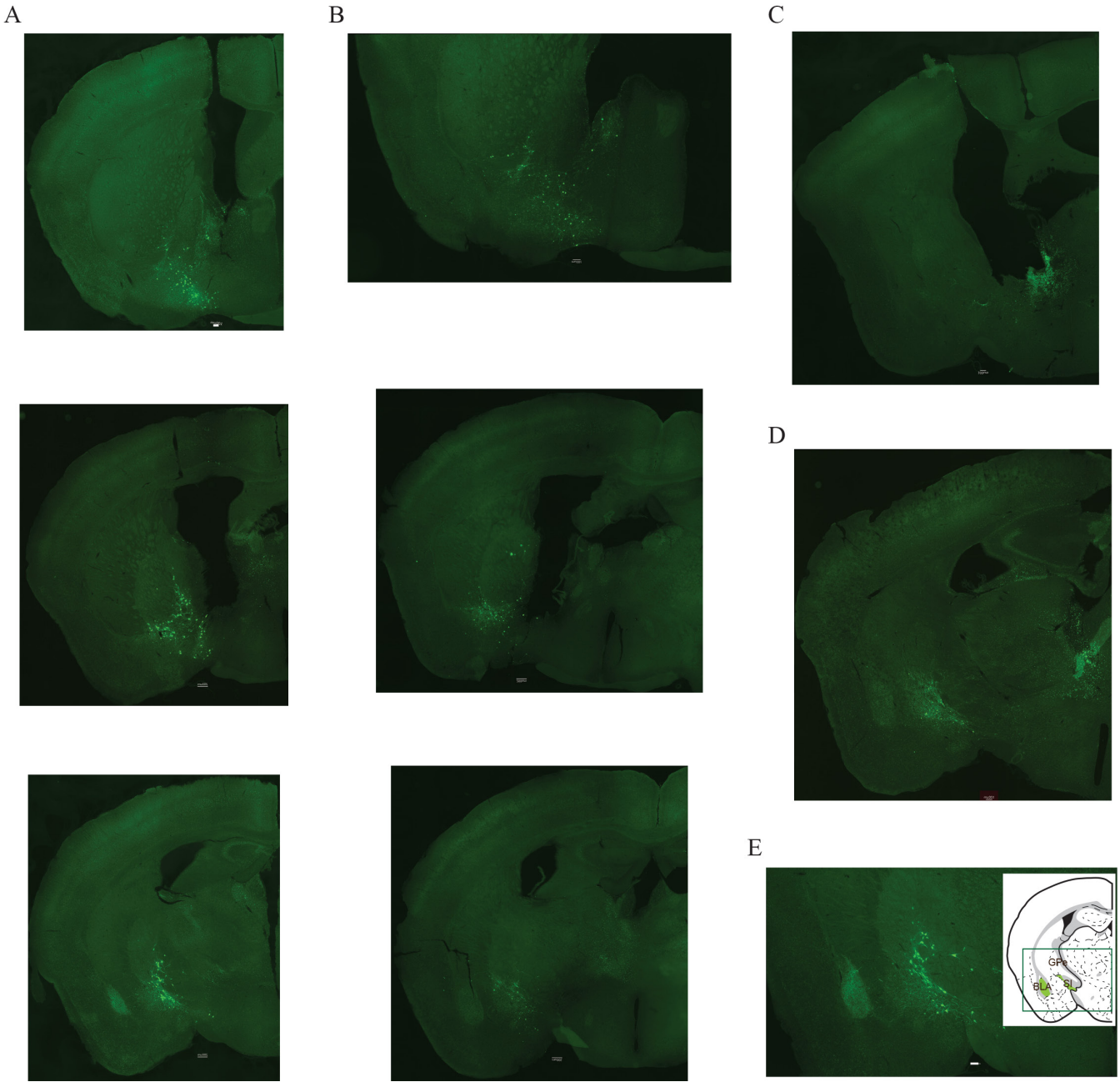

Figure S1—eYFP labeling of processes and cell bodies of cholinergic neurons transfected with eYFP virus injected in BF cholinergic space. **(A-D)** Representative injection and cannula locations of 4 animals that went through sleep experiments. **(A)** Top section is same as in (Figure 1A). Sections from an animal with unilateral eYFP injection. **(B)** Sections from an animal with unilateral ChR2-eYFP injection. **(C,D)** Sections from an animal with unilateral ChR2-eYFP injection. **(D,E)** Visualization of eYFP positive fibers across amygdaloid structures. **(E)** Same animal as in **(A)** with a unilateral eYFP injection. Scale is 100 micrometers. Inset, representative coronal section at -1.25 mm AP from Allen Brain Atlas.[57]

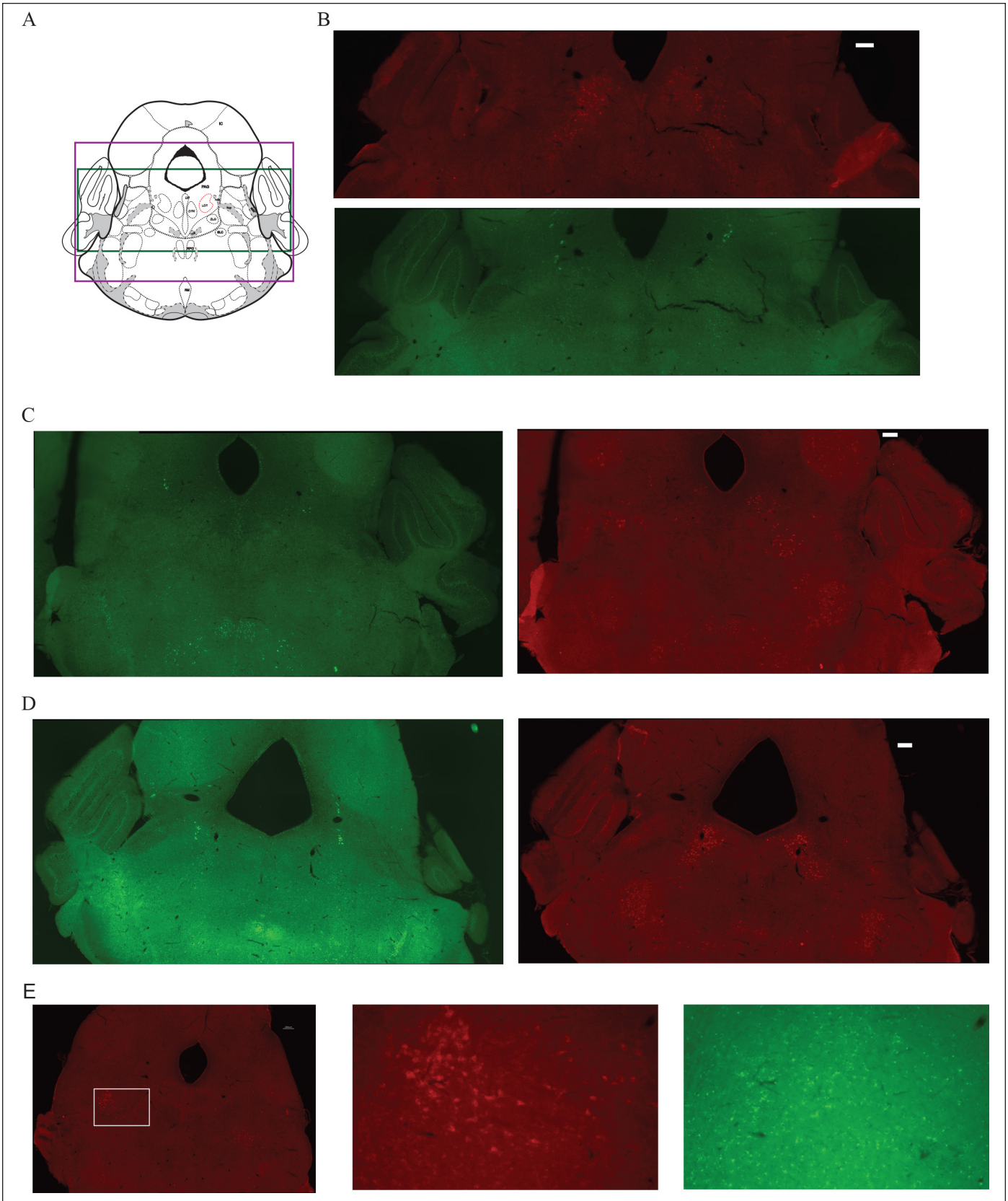

Figure S2—Lack of eYFP labeling in Brain Stem cholinergic areas. **(A)** Representative coronal section at -5.15 mm AP from Allen Brain Atlas.[57] Open boxes indicate representative locations for the pictures in **(B-D)**. **(B)** Sections from an animal with unilateral ChR2-eYFP injection. **(C)** Sections from an animal with unilateral eYFP injection. **(D,E)** Sections from an animal (same animal) with ChR2-eYFP injection. Note the un-level coronal plane in **(C-E)**. **(E)** Open box shows the zoomed-in area for the right two columns. Green, eYFP labeling. Red, ChAT staining.

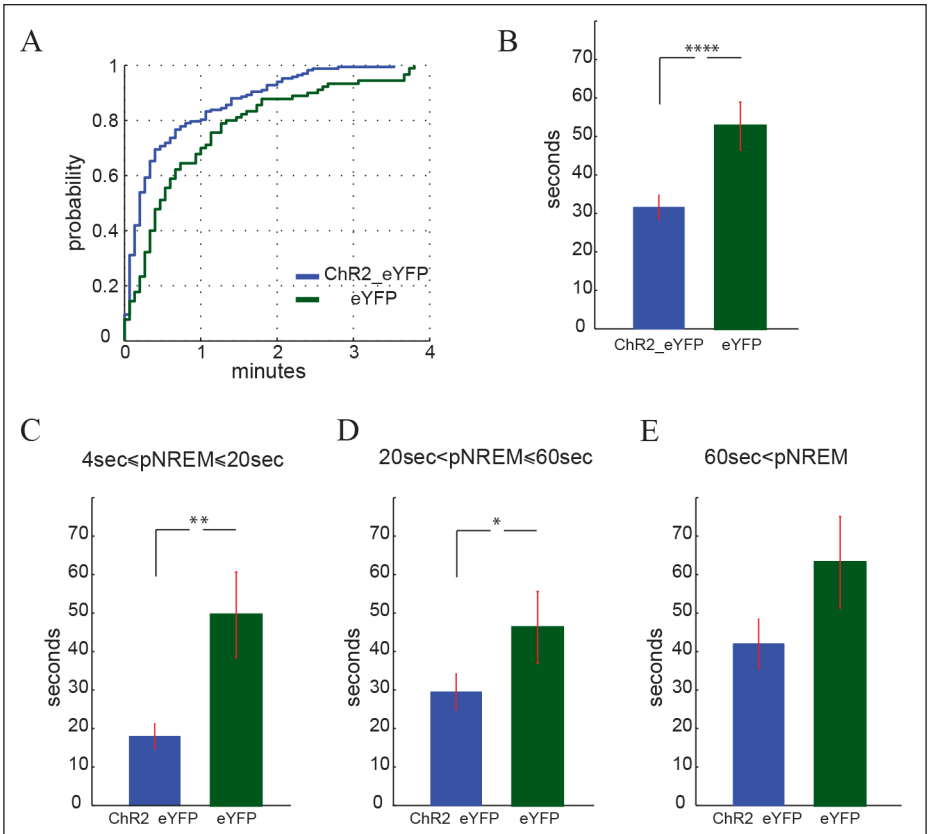

Figure S3—Effects of NREM cholinergic activation on transitions to wakefulness. **(A)** Cumulative probability distribution of NREM to wakefulness transition latencies. 167 and 90 trials for ChR2-eYFP and eYFP animals, n = 5 animals per group. **(B)** Mean (± SEM) NREM to wakefulness transition latencies. **(C-E)** Breakdown of sessions depending on the length of preceding NREM sleep. Mean (± SEM) NREM to wakefulness transition latencies. Asterisks indicate significance according to Kruskal-Wallis test. *P < 0.05. **P < 0.01. ****P < 0.0001. Note that transition latencies are referenced to the stimulation onset. *pNREM,* prior NREM sleep episode. *ChR2_eYFP,* animals transfected with ChR2-eYFP virus. *eYFP,* animals transfected with eYFP virus.

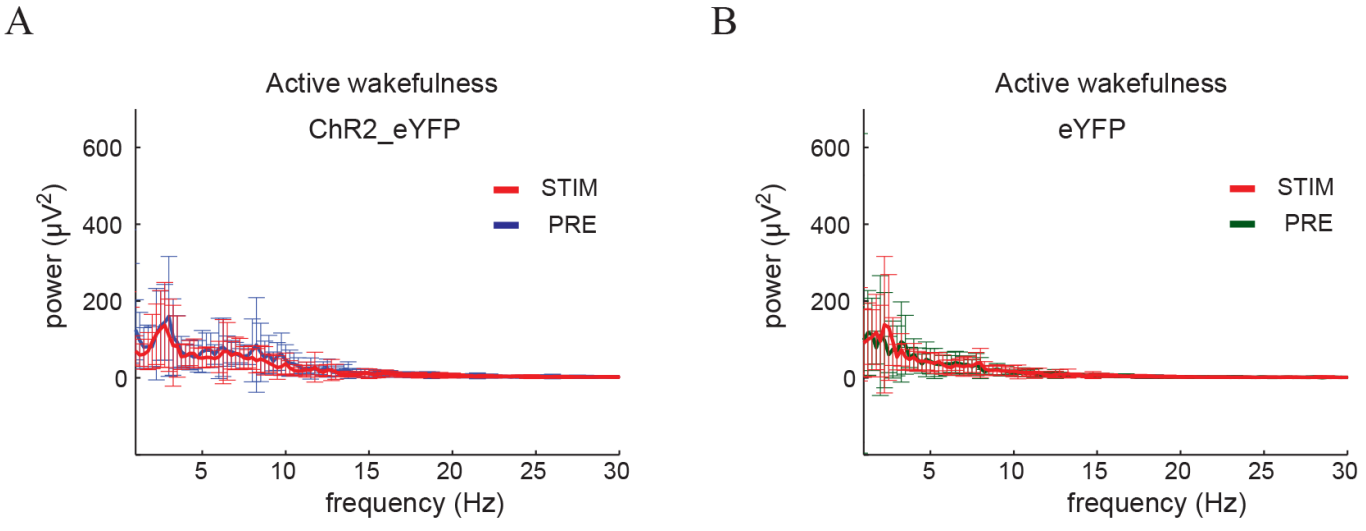

Figure S4—Optogenetic stimulation during wakefulness. **(A,B)** Spectral power across baseline (PRE) and stimulation (STIM) periods for ChR2-eYFP and eYFP animals (14 and 10 trials for ChR2-eYFP and eYFP groups, n = 3 animals per group). Error bars, standard deviation. *PRE*, 20-s preceding the stimulation onset. *STIM*, 20-s after the stimulation onset.